Applied Catalysis A: General 528 (2016) 93–103

Contents lists available at ScienceDirect

Applied Catalysis A: General

journal homepage: www.elsevier.com/locate/apcata

Feature Article

Amidase activity of phosphonate TSA-built polymer catalysts derived from organic monomers in the amidolysis of amino acid *p*-nitroanilides

Divya Mathew[a], Benny Thomas[a,b], K.S. Devaky[a,*]

[a] School of Chemical Sciences, Mahatma Gandhi University, Kottayam, 686 560, India
[b] Department of Chemistry, St. Berchmans College, Changanacherry, 686 101, India

ARTICLE INFO

Article history:
Received 25 July 2016
Received in revised form
26 September 2016
Accepted 30 September 2016
Available online 1 October 2016

Keywords:
Molecularly imprinted macromatric polymer catalyst
Transition state analogue
Imprinting efficiency
Enzyme-mimetic catalytic amidolysis

ABSTRACT

Highly crosslinked transition state analogue imprinted macromatric polymer catalysts having imidazole, carboxyl and hydroxyl functional groups in the catalytic sites were synthesized as chymotrypsin mimics using achiral organic monomers 4-vinylimidazole, methacrylic acid, allyl alcohol and phenyl-1-(N-benzyloxycarbonylamino)-2-(phenyl)ethyl phosphonate (transition state analogue of ester and amide hydrolytic reactions) as the template. The catalytic properties of the enzyme mimics were investigated in the amidolytic reactions of L-amino acid *p*-nitroanilides and correlated to the amidase activities of the catalysts derived from chiral methacryloyl-L-amino acid monomers methacryloyl-L-histidine, methacryloyl-L-aspartic acid and methacryloyl-L-serine. A two-fold enhancement in rate acceleration, substrate specificity, substrate shape-selectivity and stereoselectivity was observed for polymers made up of flexible amino acid monomers compared to the copolymers of organic monomers. The pre-polymerization complex of TSA with methacryloyl-L-amino acid monomers fabricates specific 3D-memory cavity preferentially of L-enantiomer of the TSA in the polymer matrix while the achiral organic monomers designs both L- and D- cavities The effect of crosslink density on the catalytic efficiencies of the polymer catalysts was also investigated. Replacement of allyl alcohol by vinylpyridine afforded catalyst with better enzymatic activity.

1. Introduction

Molecularly imprinted polymer catalysts (MIPs) have received considerable attention due to their thermal and pH stability and increased shelf life where natural enzymes may lose activity [1–4]. The proteolytic enzyme chymotrypsin continues to be a good model of MIP catalysts. Imidazole group of histidine residue is the essential catalytic group in the active site of the hydrolase protein chymotrypsin which cleaves the phenylalanine, tryptophan and tyrosine residues in peptide chains. Based on the theory of transition state stabilization for ester hydrolysis, phosphonic monoester TSA is generally used as a template molecule in molecular imprinting [6–12]. Even though there are many reports on MIP catalyzed esterolytic reactions, amide or peptide hydrolysis reactions using artificial enzyme mimics are less studied. We have reported the amidolysis of phenylalanine *p*-nitroanilides using phosphonate TSA imprinted copolymers of amino acid monomers-methacryloyl-L-histidine, methacryloyl-L-aspartic acid and methacryloyl-L-serine [13]. Phosphonate analogue imprinted polymers with 4-vinylimidazole [14–16], methacrylic acid [9,17] and 4-vinylpyridine [18] have been used for esterolytic reactions. The present work describes the design and synthesis of catalytically active phenyl-1-(N-benzyloxycarbonylamino)-2-(phenyl)ethyl phosphonate (TSA). The individual and combined effects of 4-vinylimidazole, methacrylic acid, allyl alcohol and 4-vinylpyridine were studied in detail.

2. Experimental

2.1. Materials and methods

Dicyclohexylcarbodiimide (DCC), ethylene glycol dimethacrylate (EGDMA) and 4-vinylpyridine (VP) were purchased from Sigma Aldrich, USA. Z-L-Phenylalanine, methacrylic acid (MAA), allyl alcohol (AA), benzylcarbamate, triphenyl phosphite and pheny-

* Corresponding author at: School of Chemical Sciences, Mahatma Gandhi University, Priyadarshini Hills, P.O Kottayam, 686 560, Kerala, India.
E-mail address: ksdevakyscs@yahoo.com (K.S. Devaky).

http://dx.doi.org/10.1016/j.apcata.2016.09.020
0926-860X/

lacetaldehyde were purchased from SRL, Mumbai. All chemicals used, other than listed above were from local suppliers, which were purified prior to use by following the standard procedures. IR spectra were recorded on a Shimadzu FT-IR-8400S spectrophotometer. Kinetic studies were performed using Shimadzu UV 2450 spectrophotometer. JEOL JSM6390 SEM analyzer was used for SEM analysis. 1H NMR spectra were taken using Bruker Advance DPX–300 MHz FT-NMR spectrometer in $CDCl_3$. BET analyzer used was Thermo Fisher Scientific Surface Analyzer V-230 50/60 Hz.

2.2. Synthesis of TSA (Phenyl-1-(N-benzyloxycarbonylamino)-2-(phenyl)ethyl phosphonate)

The transition state analogue was synthesized by refluxing 4.1 mL, 13.2 mmol triphenyl phosphite, 2.0 g, 13.2 mmol benzyl carbamate, 2.38 mL, 19.8 mmol phenylacetaldehyde and 2.0 mL glacial acetic acid for 4 h at 100 °C in an oil bath. FTIR: –1301 cm^{-1}(P=O stretching), 946 cm^{-1}(P-OH stretching) and 1252 cm^{-1} (P-O-benzyl stretching) [13].

2.3. Synthesis of monomer 4-vinylimidazole

The functional monomer 4-vinyimidazole (VIm) was prepared from urocanic acid as per the reported procedure [14].

2.4. Synthesis of TSA imprinted enzyme mimics and non-imprinted control polymers

The polymer catalyst **P1a** was prepared by radical initiated bulk polymerization of 752 mg, 8.0 mmol, of monomer 4-vinylimidazole (VIm) and 396 mg, 2.0 mmol, of the crosslinking agent EGDMA in presence of 1.8 g, 4.0 mmol TSA in 40 mL DMSO for 6 h at 80 °C. The template was completely leached out by washing with methanol and then subjected to Soxhlet extraction with chloroform. The polymer obtained was collected and dried over vacuum. Enzyme mimics **P1b-P3e** were also synthesized as per the same procedure by varying the molar ratios of monomer and crosslinker. The corresponding non-imprinted control polymers **CPs** were also prepared by the same procedure in the absence of TSA.

2.5. Synthesis of the substrates phenylalanine p-nitroanilides

The substrate Z-L-phenylalanine *p*-nitroanilide was synthesized by DCC coupling of a suspension of 299 mg, 1 mmol of Z-L-phenylalanine and 138 mg, 1 mmol of *p*-nitroaniline in 30 mL ethyl acetate. The dicyclohexylurea (DCU) formed was filtered off and the filtrate was evaporated in vacuum. The residue obtained was recrystallized from hot ethanol containing 1% acetic acid.

2.6. Amidolysis of phenylalanine p-nitroanilides using TSA imprinted and non-imprinted enzyme mimics

In a reagent bottle, to a suspension of 10 mg, 0.012 mmol of the polymer catalyst **P1a** in 5 mL acetonitrile-Tris HCl buffer (1:9 by volume, pH 7.75), 503 mg, 1.2 mmol of the substrate Z-Phe-PNA in 50 mL acetonitrile was added. The reaction mixture was placed in a water bath shaker at 45 °C and shaken gently. Amidolysis of Z-Phe-PNA was followed spectrophotometrically by monitoring the absorbance of released *p*-nitroaniline at 374 nm. A blank reaction was also carried out in the absence of the enzyme mimic. From the absorbance data, the rate constants and percentage amidolysis were evaluated. Amidase activity of the mimics **P1b-P3d** was evaluated in a similar manner.

All the experiments were repeated 4 times and the average of the results were reported here. The error of the results lies within ±5%. Since the heterogeneity of the polymer catalysts and solvation problems, the results show some deviations in reproducibility.

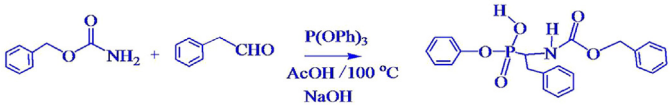

Scheme 1. Synthesis of the phosphonate TSA.

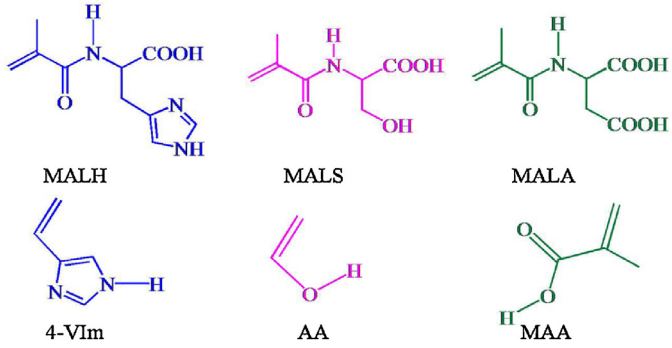

Fig. 1. Structure of methacrylated amino acid monomers and their organic analogues.

3. Results and discussion

3.1. Synthesis of TSA-built and non-built polymer catalysts

The TSA, which has more structural resemblance with the substrate Z-L-Phe-PNA was synthesized using triphenyl phosphite, benzyl carbamate and phenylacetaldehyde (Scheme 1). The TSA synthesized possesses N-benzyloxycarbonyl (Z) protecting group of the substrate and the "specificity determinant"- $C_6H_5CH_2$ group – complementary to the hydrophobic pocket of chymotrypsin CT [19,20]. The TSA was characterized by FTIR and NMR spectroscopic techniques.

The methacrylated L-amino acid monomers – methacryloyl-L-histidine (MALH), methacryloyl-L-aspartic acid (MALA) and methacryloyl-L-serine (MALS) – were synthesized by Schotten-Bauman reaction [5] and the organic monomer 4-vinylimidazole was prepared from urocanic acid [14].

The TSA imprinted polymers were prepared by radical initiated bulk polymerization method using the functional monomers, template TSA and the crosslinker EGDMA as per the reported procedure. The structure of the methacrylated L-amino acid monomers and their organic analogues used are shown in Fig. 1 and the details of polymer synthesis are given in Table 1.

The monofunctional mimics **(P1a-P1c)**, bifunctional mimics **(P2a-P2c)** and trifunctional mimics **(P3a-P3d)** were synthesized using the functional monomers 4-VIm/MAA/AA with EGDMA. In all enzyme mimics –mono/bi/trifunctional mimics, the concentration of the print molecule and total concentration of monomers is taken fixed as 1:2. Since the allyl alcohol containing polymer catalysts were found to be less efficient in amidolytic reactions, we prepared trifunctional mimic **P3e** by replacing allyl alcohol by vinylpyridine.

The corresponding non-imprinted control polymers **(CPs)** were also synthesized in the same molar ratios of monomers and the crosslinker without the TSA molecule. The total functional group contents were estimated by titration method as per the reported procedures.

The trifunctional mimic (**C3**) comprising of amino acid monomers was synthesized in presence of EGDMA crosslinker (90%) and TSA. The total functional group content (TFGC) was estimated using ninhydrin reagent [5].

Table 1
Details of the synthesis of polymer catalysts.

Polymer Catalysts		FunctionalMonomers	%Crosslinker	TFGC
Monofunctional	P1a	4-VIm	20%	1.187
	P1b	MAA	20%	1.156
	P1c	AA	20%	1.144
Bifunctional	P2a	4-VIm/MAA	20%	1.021
	P2b	4-VIm/AA	20%	1.078
	P2c	MAA/AA	20%	1.072
Trifunctional	P3a	4-VIm/MAA/AA	90%	0.643
	P3b	4-VIm/MAA/AA	10%	1.084
	P3c	4-VIm/MAA/AA	20%	1.065
	P3d	4-VIm/MAA/AA	30%	1.037
	P3e	4-VIm/MAA/4-VP	20%	1.072

Table 2
Details of BET surface area analysis and TSA rebinding studies.

Enzyme mimics	Surface area (m^2/g)	Pore volume (cm^3/g)	[TSA rebound] mmol/g
C3	311.55	0.898	0.184
P3c	267.16	0.770	0.358
P3e	285.37	0.823	0.364

Table 3
Catalytic amidolysis and effect of the extent of EGDMA crosslinking.

Kinetic parameters/Catalysts	Trifunctional Mimics				
	P3a	P3b	P3c	P3d	C3
k_{acc}	6.78	21.62	35.42	23.56	75.38
k_{im}	1.02	1.43	2.12	1.37	4.22
S_t(h)	nd	50	24	70	22

St–time for saturation, nd– not observed saturation even after several days, all kinetic parameters within the limit ±5%.

Proficient pre-organization is essential for successful imprinting [21–24]; from the *rac*-TSA synthesized, the achiral organic monomers (4-VIm, MAA and AA) having the functional groups present in active site of chymotrypsin –imidazole, carboxyl and hydroxyl- formed TSA-monomer pre-polymerization complex with both L- and D-TSA. A suitable crosslinker with sufficient crosslink density freezes the stable, H-bonded TSA-monomer pre-polymerization complex into rigid polymer matrix and after polymerization, removal of TSA leaves behind its '3D- imprints' lined with catalytic entities. The 'specificity determinant' $C_6H_5CH_2$ group of TSA, designs the hydrophobic pocket in the polymer matrix. The pre-polymerization complexes (PPC) formed are depicted in Scheme 2. The PPC of methacrylated L-amino acid monomers (**a**) and that of their organic analogues-vinylimidazole, methacrylic acid and allyl alcohol (**b**) are held together by H-bonding interactions. The chiral L-amino acid monomers form PPC selectively with L-TSA and fabricate catalytic cavities with L-configuration in the polymer matrix. But, the achiral organic monomers form PPC with TSA having both L- and D- configurations. The π-stacking interaction of pyridine moiety with the specificity determinant $C_6H_5CH_2$ group of TSA makes the PPC (**c**) more stable.

The structural difference between the imprinted polymers become more obvious upon assessment of the data received from BET surface area analysis (Table 2). The higher surface area of imprinted polymers is indicative of distribution of pores (cavities) and higher binding capacity. The pore volume measurements show that **C3** has a maximum pore volume of 0.898 cm^3/g [25].

The amount of bound TSA was quantitatively eluted by Soxhlet extraction using chloroform and the TSA in the eluate was estimated spectrophotometrically at 245 nm. The specific rebinding of the TSA molecules by the imprinted polymers **C3**, **P3c** and **P3e** were carried and the amount of TSA rebound was determined using the equation, $\boldsymbol{Q_e} = \frac{(\boldsymbol{C_0}-\boldsymbol{C_e})\boldsymbol{V}}{\boldsymbol{M}}$ where $\boldsymbol{C_0}$ (mmol/g) and $\boldsymbol{C_e}$ (mmol/g) are the initial and equilibrium concentration, **V** (L) is the volume of the TSA solution and **M** (g) is the weight of the imprinted polymer. The polymers could rebind the TSA molecules effectively and the amounts of TSA rebound evaluated were given in Table 2. The two values obtained were in good agreement.

The morphological differences of imprinted and non-imprinted polymer catalysts were assessed by SEM analysis. The SEM picture of **C3** and **P3e** is full of cavities by the removal of the imprinted phosphonate TSA. But, the surface of the corresponding non-imprinted control polymers is almost smooth without cavities (Fig. 2).

3.2. Evaluation of the kinetics of catalytic amidolysis

Amidolysis proceeds through a higher energy tetrahedral oxyanion intermediate and the **"shape-selective-stabilization"** of the unstable intermediate in the memorized cavity fabricated by the print molecule leads to the rate enhancement with the enzyme mimics. The key acceleration processes of catalytic amidolysis are substrate binding process, stabilization of the T.S of the amidolytic reaction and finally release of the product. The amidolysis of Z-L-Phe-PNA was found to be too slow in aqueous medium (0.16×10^{-8} min^{-1}) and in Tris HCl buffer at room temperature (0.98×10^{-5} min^{-1}).The amidolysis was carried out in 1:9 acetonitrile–Tris HCl buffer of pH 7.75 at 45 °C which is found to be the optimum temperature and the kinetics of amidolysis with catalysts was evaluated spectrophotometrically at 374 nm by monitoring the amount of *p*-nitroaniline released. A blank experiment was also carried out under similar conditions without the catalysts. The pseudo-first order rate constants were obtained from the following equation: $\boldsymbol{ln}\left[\frac{\boldsymbol{A_{max}}}{\boldsymbol{A_{max}}-\boldsymbol{A_t}}\right] = \boldsymbol{kt}$ where $\boldsymbol{A_{max}}$ is the absorbance of *p*-nitroaniline at infinite time, $\boldsymbol{A_t}$ is the absorbance of *p*-nitroaniline at time **t** and $\boldsymbol{k}$ is the pseudo-first-order rate constant. At 45 °C, in 1:9 MeCN–Tris HCl buffer of pH 7.75 the rate constant for the blank is found to be 0.52×10^{-4} min^{-1}. The rate acceleration $\boldsymbol{k_{acc}}$ values of the polymer catalysts were evaluated in terms of the ratio $\boldsymbol{k_{obs.}}/\boldsymbol{k_{uncat.}}$ and the imprinting efficiency $\boldsymbol{k_{im}}$ of the polymer catalysts is expressed in terms of $\boldsymbol{k_{MIP}}/\boldsymbol{k_{CP}}$. The possible mechanism for the amidolysis catalyzed by **C3** is depicted in Scheme 3.

In our previous study of the amidolysis of Z-L-Phe-PNA using trifunctional imprinted polymer catalyst **(C3)** comprises of methacrylated L-amino acid monomers; it was found that the 90% EGDMA crosslinking is essential to preserve the 3D-geometry of the imprint and to facilitate the uptake of the substrate Z-L-Phe-PNA molecule [13]. But, the rate acceleration exhibited by trifunctional mimic **P3a** comprises of the organic analogues of amino acid monomers polymerized with 90% EGDMA crosslinks is only 6.78, compared to the $\boldsymbol{k_{acc}}$ value 75.38 for **C3**, 90% EGDMA crosslinked trifunctional mimic made up of methacrylated L-amino acid monomers. Further, the imprinting efficiency values $\boldsymbol{k_{im}}$ evaluated are 1.02 (**P3a**) and 4.22 (**C3**) indicating poor catalytic efficiency of **P3a**. Moreover **P3a** did not exhibit any saturation in its amidase

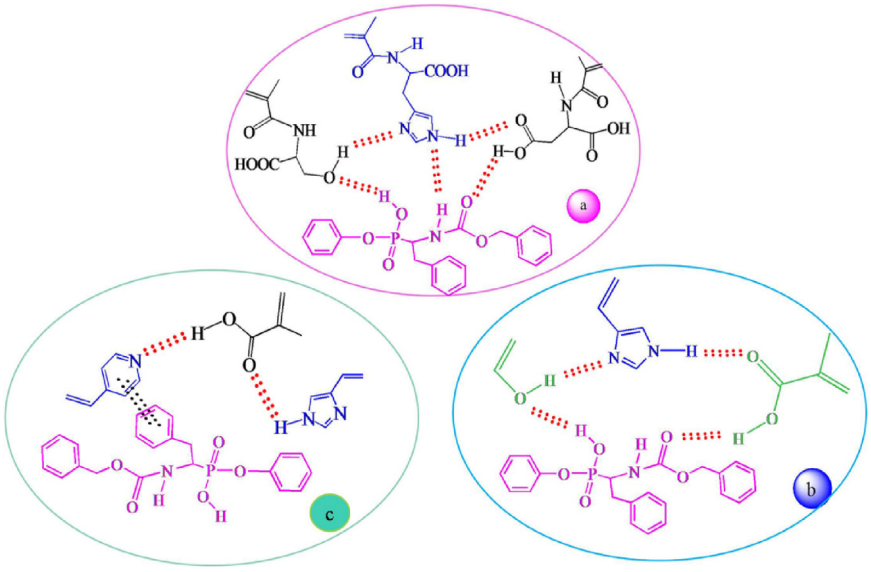

Scheme 2. Pre-polymerization complexes.

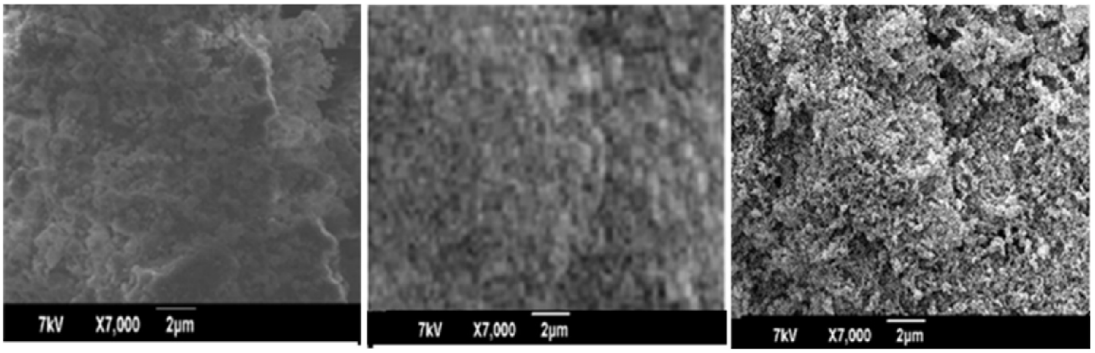

Fig. 2. SEM pictures a) **P3c,** b) **P3e** and c) **C3**.

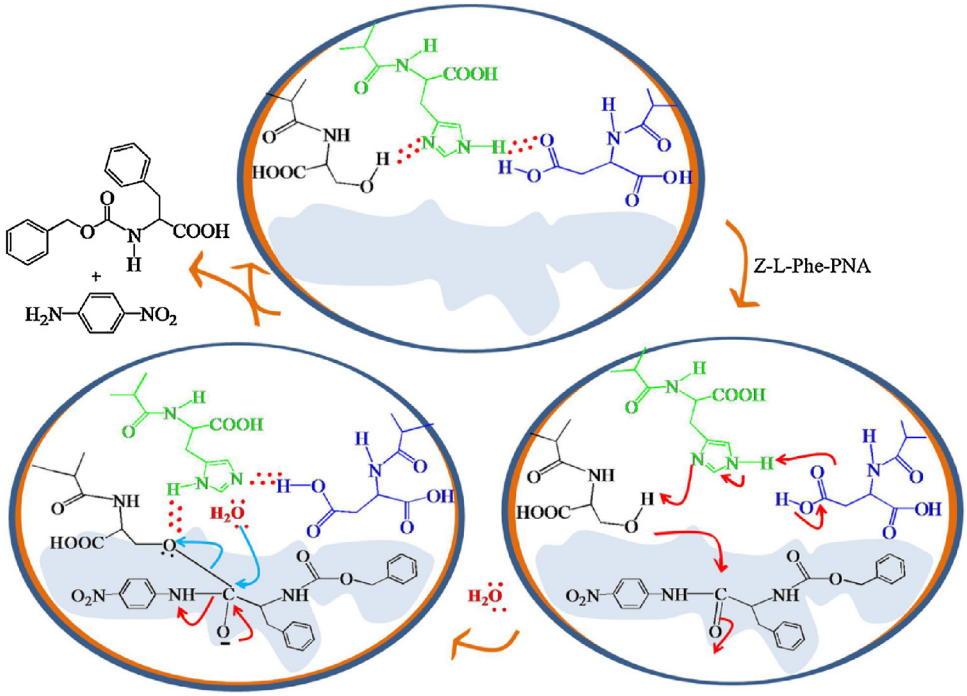

Scheme 3. Catalytic amidolysis of Z-L-Phe-PNA using **C3**.

Table 4
Co-operative effect of functional monomers and catalytic amidolysis.

Catalysts with L-amino acid monomers				Catalysts with organic monomers			
Enzyme mimic	k_{acc}	k_{im}	S_t(h)	Enzyme mimic	k_{acc}	k_{im}	S_t(h)
C1a	29.62	2.37	50	P1a	10.46	1.05	70
C1b	12.50	1.12	120	P1b	6.52	1.03	nd
C1c	15.00	1.08	120	P1c	6.34	1.02	nd
C2a	41.53	2.60	40	P2a	17.78	1.06	45
C2b	45.77	2.74	35	P2b	14.08	1.04	45
C2c	15.96	1.15	120	P2c	7.66	1.01	nd
C3	75.38	4.22	22	P3c	35.68	2.12	24

Allkineticparameters within the limit ±5%.

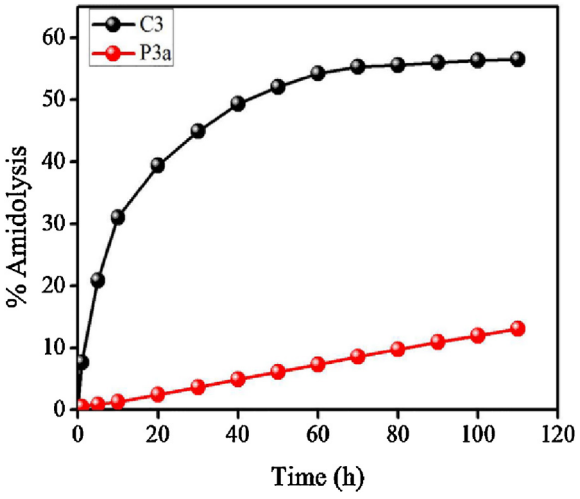

Fig. 3. % Amidolysis vs time.

activity even after several days. The lack of well-defined substrate recognition sites in the matrix of **P3a** as a consequence of higher rigidity provided by 90% EGDMA crosslinks may be the reason for its poor catalytic activity.

Since the functional groups in the organic monomers VIm, MAA and AA are less flexible compared to the amino acid monomers MALH, MALA and MALS, the super crosslinked networks of EGDMA makes the polymer highly rigid to impede the release of the print molecule and uptake of the substrate molecule and catalysis was not observed in the hydrolytic reaction (Fig. 3).

There are some reports in which imprinted catalysts have been prepared with low degree of crosslinking [26,27,32]. Hence in the case of trifunctional mimics of organic monomers, crosslink density in the range of 10–30% (**P3b-P3d**) was used to freeze the catalytic functions intact and to preserve the exact geometry of the imprint. The amidolysis was carried out in the framework of Michaelis-Menten kinetics using polymers **P3b-P3d** with 10, 20 and 30% EGDMA crosslinks and the results are given in Table 3. The rate acceleration value exhibited by **P3b** was observed to be 21.62. The trifunctional mimic **P3c** with 20% EGDMA crosslinks was observed to be the best polymer catalyst with k_{acc}, k_{im} and S_t values 35.42, 2.12 and one day respectively. On further increase in crosslink density to 30% decelerates the rate acceleration (23.56) and imprinting efficiency (1.37). The **P3c** polymer showed 5.2 times rate acceleration than **P3a** polymer; but, showed 2.1 times lower rate acceleration compared to the trifunctional mimic **C3** comprises of amino acid monomers. The methacrylated L-amino acid monomers selectively forms TSA-monomer pre-polymerization complex with L-TSA over D-TSA and leaves out memory cavities with L-configuration and selectively binds the substrate Z-L-Phe-PNA. But, due to the achiral nature of organic monomers, the polymer matrix of P-type polymer catalysts may be composed of both L- and D-cavities.

Table 5
Co-operative effect of functional monomers in the trifunctional mimics in the catalytic amidolysis-a comparison.

Enzyme mimic	k_{acc}	k_{im}	S_t(h)
C3	75.38	4.22	22
P3c	35.68	2.12	24
P3e	44.60	2.46	20

Allkineticparameters within the limit ±5%.

3.3. Co-operative effect of functional monomers on amidolysis

The number, strength and orientation of the functional groups and their interactions with the print molecule are the key factors in determining the shape-selective binding of the substrate molecules. The individual and combined effects of imidazole, carboxyl and hydroxyl groups of methacrylated L-amino acid monomers in the chymotrypsin mimics on the amidolysis of Z-L-Phe-PNA were demonstrated in detail in our previous paper and it was observed that only the mimics containing imidazole moieties exhibit chymotrypsin like behaviour towards Z-L-Phe-PNA. The same effect was observed for polymer catalysts with organic monomers (Table 4).

Among the monofunctional catalysts, the highest rate acceleration k_{acc} value (10.46) is observed for **P1a** polymer with imidazole moieties. The bifunctional mimic **P2a** with imidazole and carboxylic groups exhibited enhanced [k_{cat}/k_{uncat}] value of 17.78 and **P2b** with imidazole and hydroxyl residues showed [k_{cat}/k_{uncat}]value of 14.08. But bifunctional mimic **P2c** with carboxyl and hydroxyl residues is found to be catalytically poor with k_{acc} value of 7.66. The trifunctional polymer catalyst **P3c** showed the maximum k_{acc} value 35.68. The polymer catalysts formed from organic monomers showed lower k_{acc} values compared to the catalysts derived from amino acid monomers. The ratios $k_{acc}^{C1a}/k_{acc}^{P1a}$, $k_{acc}^{C2a}/k_{acc}^{P2a}$, $k_{acc}^{C2b}/k_{acc}^{P2b}$ and $k_{acc}^{C3c}/k_{acc}^{P3c}$ are 2.83, 2.34, 3.25 and 2.11 respectively. Further the ratio $k_{acc}^{C1c}/k_{acc}^{P1c}$ and $k_{acc}^{C2c}/k_{acc}^{P2c}$ are 2.37 and 2.08. These results reveal that the catalytic property contributed by the hydroxyl group of allyl alcohol is low in the amidolytic reaction compared to serine.

The catalytic amidolysis of the substrate Z-L-Phe-PNA using **P3c** comprising of rigid organic monomers is depicted in Scheme 4.

Since the polymer catalysts with allyl alcohol showed poor nucleophilicity compared to serine in the amidolytic reaction, we synthesized a trifunctional polymer catalyst **P3e** by replacing allyl alcohol by vinylpyridine. It is reported that pyridine units provide better nucleophilic sites in chymotrypsin mimics for esterolytic reactions [18]. The mimic **P3e** exhibited a k_{acc} value of 44.60. The ratio $k_{acc}^{P3e}/k_{acc}^{P3c}$ was found to be 1.25. The selective binding of substrate in the catalytic cavity of **P3e** is expected to be facilitated by the π stacking interactions of pyridine moieties. The proton

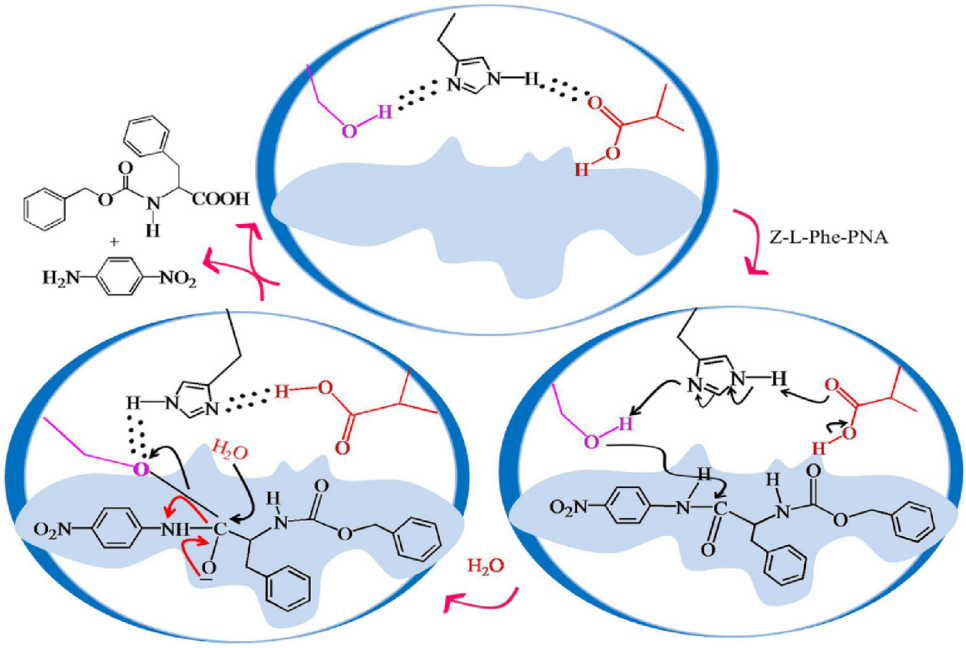

Scheme 4. Amidolysis of Z-L-Phe-PNA using enzyme mimic **P3c**.

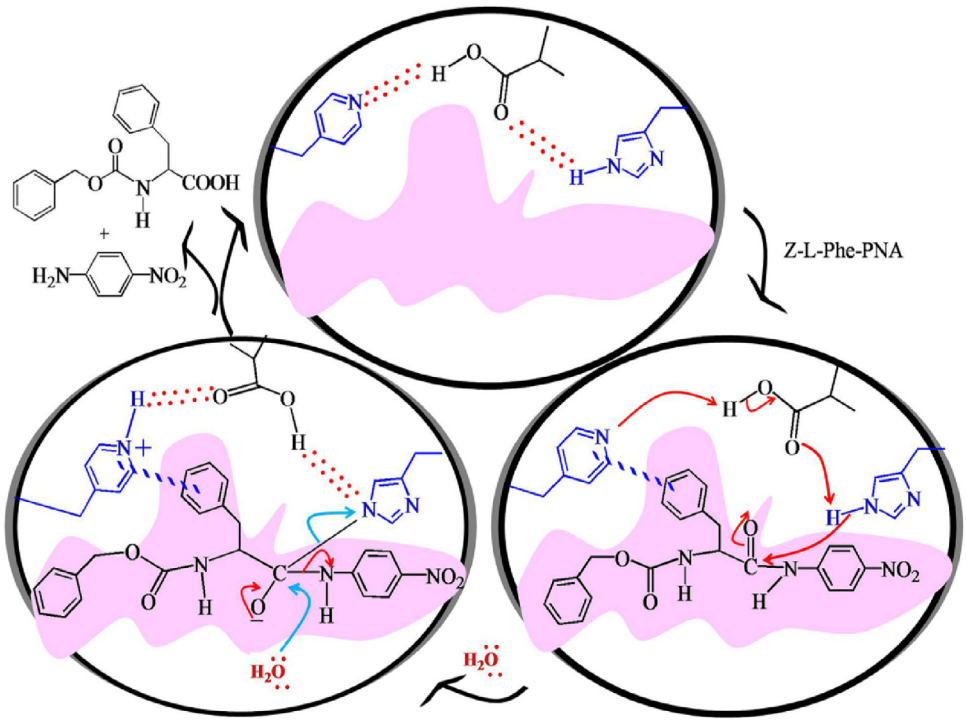

Scheme 5. Amidolysis of Z-L-Phe-PNA using enzyme mimic **P3e**.

shuttle between pyridine and carboxylic functions at the active sites increases the nucleophilicity of imidazole units. Moreover, **P3e** attains saturation within a shorter time period (20 h) than **P3c** (24 h). The proposed mechanism is depicted in Scheme 5.

A comparison of the amidase activities of the trifunctional mimics **P3c** and **P3e** derived from achiral organic monomers and **C3** made from chiral amino acid monomers is listed in Table 5. Thus, for polymers comprises of amino acid monomers, the rate enhancement is observed only with higher extreme crosslink density. But, for the polymers of organic monomers, a rate enhancement is observed, in the lower range of crosslink density (20%).

3.4. *Effect of pH on the amidase activities of the trifunctional enzyme mimics*

Amidolysis of Z-L-Phe-PNA was carried out in the pH range 6.0–8. The polymers **P3c, P3e** and **C3** follow the same pH profile that it exhibits an optimum rate at pH 7.75 (Fig. 4). The mechanism

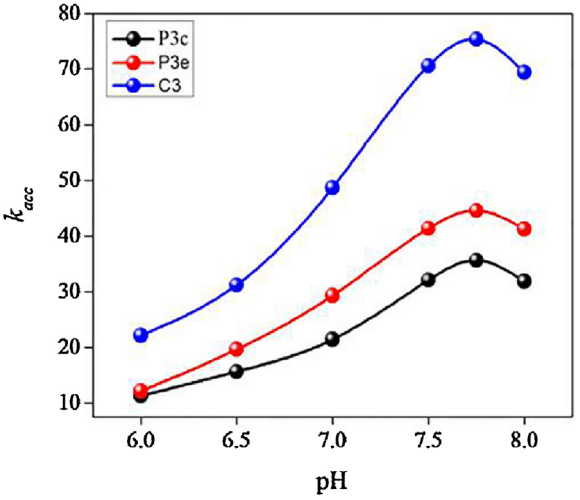

Fig. 4. Effect of pH on catalytic amidolysis.

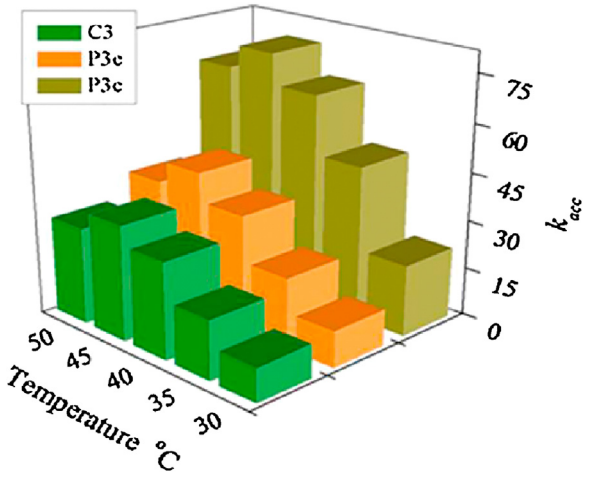

Fig. 5. Effect of temperature on rate acceleration.

shows that the catalytic activity of the enzyme mimics arises due to the cooperative effect of neutral imidazole groups and most of the imidazole units are non-protonated at the optimum pH 7.75. As the pH of the reaction medium decreases protonation of imidazole nitrogen decreases the nucleophilicity. At higher pH of the reaction medium, the rate of uncatalyzed reaction increased due to the increased concentration of hydroxyl ions. At higher pH of the reaction medium, the polymer bound negatively charged carboxylic acid groups provides electrostatic exclusion of nucleophilic OH- from polymer-substrate complex resulting in the inhibition [9]. At higher pH of the reaction medium, the rate of uncatalyzed reaction increased due to the increased concentration of hydroxyl ions.

3.5. Effect of temperature on the catalytic activities of the trifunctional polymer catalysts

To investigate the optimum temperature for catalytic amidolysis, the reaction was carried out at different temperatures (30, 35, 40, 45 and 50 °C) using the mimics **P3c**, **P3e** and **C3** and the results are given in Fig. 5. It is reported that, as temperature increases, the catalytic sites become more accessible and exhibit higher catalytic efficiency [3]. The time taken for saturation in amidase activity of the polymer catalyst is also found to be decreasing as temperature increases (Fig. 6).

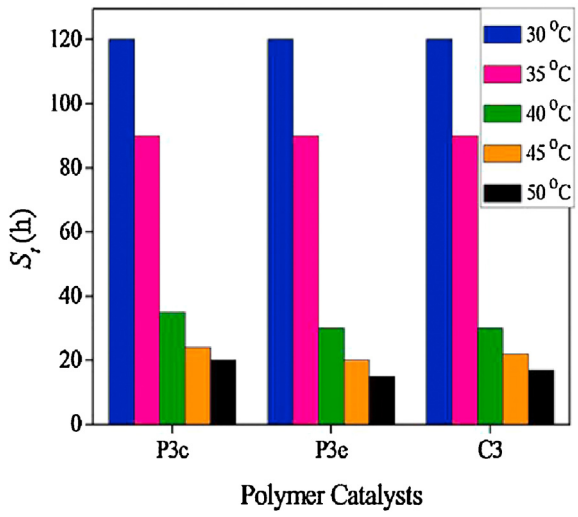

Fig. 6. Effect of temperature on saturation time.

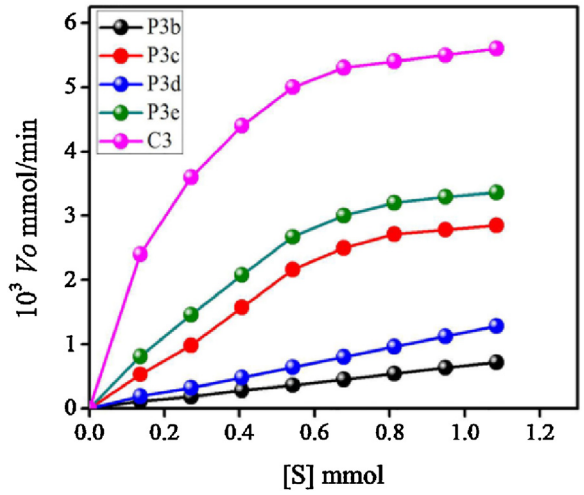

Fig. 7. Michaelis- Menten plots.

3.6. Michaelis- Menten kinetics of polymers

The Michaelis-Menten kinetic studies were carried using the polymer catalysts **P1b**-**P3e** to evaluate their substrate affinity towards Z-L-Phe-PNA in the enzyme-mimetic catalytic amidolysis and a comparison was made with the polymer catalysts made up of L-amino acid monomers [1,5,28,29]. Different enzyme-substrate concentrations were taken (1:25 to 1:150). The Michaelis- Menten plots for the trifunctional polymer catalysts **P3b**-**P3e** are shown in Fig. 7.

The competence of the polymer catalyst to mimic natural chymotrypsin has been evaluated in terms of substrate affinity of the polymer catalysts from the double reciprocal plots for the amidolytic reaction (Fig. 8).

The enzyme characteristics- K_m, V_{max}/K_m and k_{cat}/K_m- evaluated are given in Table 6. Both **P3c** and **P3e** are found to be obeying Michaelis- Menten kinetics with K_m values 1.419 and 1.151 mmol respectively. The ratio K_m^{P3c}/K_m^{P3e} was observed to be 1.23 strongly supporting the π-stacking interactions of pyridine moiety. The mimic **C3** exhibited more pronounced initial burst kinetics and saturation than **P3c** and **P3e**. The ratios K_m^{P3c}/K_m^{C3} and K_m^{P3e}/K_m^{C3} were found to be 4.26 and 5.26. Specific stereochemical "memory" of L-configuration due to the presence of L-amino acid monomers is responsible for the higher substrate specificity of the mimic **C3**.

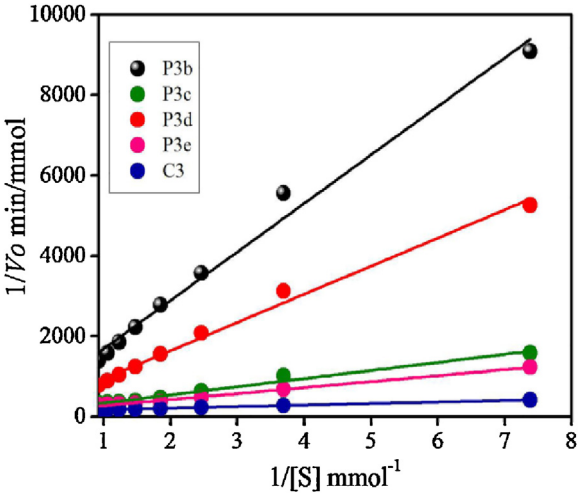

Fig. 8. Lineweaver-Burk plots.

Table 6
Michaelis-Menten kinetics for the copolymers of amino acid monomers.

Trifunctionalpolymer catalysts	K_m(mmol)	$10^3 V_{max}/K_m$(min^{-1})	k_{cat}/K_m(mmol/min)
C3	0.27	26.74	4.934
P3b	2.516	0.829	0.153
P3c	1.419	4.956	0.914
P3d	2.890	1.427	0.263
P3e	1.151	6.718	1.239

Allkinetic parameters within the limit ±5%.

CM:- *Chymotrypsin mimic;* **PNA:-** *Substrate Phenylalanine p-nitroanilide;* **CM.PNA:-***Enzyme mimic–Substrate complex;* **P:-** *Product.*

Scheme 6. Simplified reaction process of amidolysis with TSA imprinted polymer catalyst.

The polymer catalysts **P3b** and **P3d** from organic monomers do not obey Michaelis- Menten kinetics and behave like uncatalyzed reaction. The polymer **P3b** having lower EGDMA crosslinking (10%) is not capable of preserving the exact geometry of the imprint and **P3d** with higher crosslink density (30%) is having highly rigid polymer network reducing the accessibility of the catalytic sites to the substrate molecule.

3.7. Enantioselective amidolysis

The substrate stereospecificity of the mimics **P3c** and **P3e** were investigated in the amidolysis of Z-L/D-Phe PNAs [9,17,30]. The substrate stereospecificity is evaluated in terms of $\boldsymbol{k^L_{acc}/k^D_{acc}}$, $\boldsymbol{K^D_m/K^L_m}$, $\Delta\left(\Delta \boldsymbol{G^{\#}_{binding}}\right)$ and $\Delta\left(\Delta \boldsymbol{G^{\#}_{[C.S]}}\right)$ and compared with the mimic **C3** [26,27]. The activation free energy $\Delta\left(\Delta \boldsymbol{G^{\#}_{binding}}\right)$ of the shape-selective binding of substrate Z-L-Phe-PNA is evaluated as $-\boldsymbol{RTln}\left(\frac{K^D_m}{K^L_m}\right)$ and the difference of activation free energy $\Delta\left(\Delta \boldsymbol{G^{\#}_{[C.S]}}\right)$ as $-\boldsymbol{RTln}\left(\frac{k^L_{acc}}{k^D_{acc}}\right)$ in the frame work of Michaelis-Menten kinetics (Scheme 6).

Since the racemic phosphonate TSA, phenyl-1-(N-benzyloxycarbonylamino)-2-(phenyl)ethyl phosphonate was used as the print molecule for the synthesis of all the mimics, only **C3** with methacryloyl-L-amino acid residues can exhibit

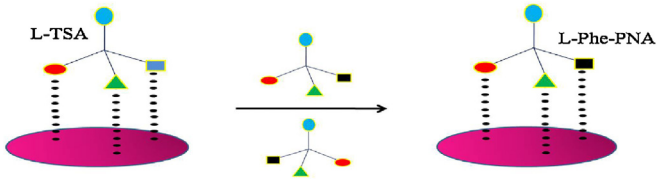

Fig. 9. Enantioselective binding of substrate by imprinted polymer.

enantioselectivity towards L-substrates. If an optically active template is used as TSA for imprinting, the polymer catalysts cause enantiomers to react at different rates. Chymotrypsin exhibits stereochemical specificity that they catalyze the reactions of L-amino acid esters or amides. It has been reported that the selective stabilization of one particular complex conformation should have a superficial influence on the enantioselectivity of the enzyme mimic (Fig. 9).

It is worth emphasizing that the chymotrypsin mimic **C3**, a trifunctional polymer catalyst of L-amino acid monomers, essentially incorporates the L-Phe-PNA primarily over the D-Phe-PNA to form the catalyst–substrate complex with $\boldsymbol{K^D_m/K^L_m} = 10.59$ and hydrolyzes the L-Phe-PNA competently with $\boldsymbol{k^L_{acc}/k^D_{acc}} = 7.56$. Thus, the enzyme mimic **C3** have memory cavities with the shape of L-TSA, and show proficient substrate-stereospecific amidolysis of Z-L-Phe-PNA through shape-selective binding of the substrate into its recognition sites. The $\boldsymbol{K^D_m/K^L_m}$ and $\boldsymbol{k^L_{acc}/k^D_{acc}}$ values of **P3c** (1.03, 1.02) and **P3e** (1.05 and 1.03) indicate that these polymers possess little enantioselectivity. This result probably came from the presence of both Land D-cavities in the polymer matrix.

Concerning the substrate-binding affinity $\boldsymbol{K^{-1}_m}$ of the polymer catalysts in the catalyst-substrate complex formation, the negative activation free energy $\boldsymbol{\Delta G^{\#}_{binding}} = -\boldsymbol{RTlnK^{-1}_m}$ indicates the non-barrier of the substrate-binding process. The $\boldsymbol{\Delta G^{\#}_{binding}}$ of **C3** for Z-L-Phe-PNA and Z-D-Phe-PNA were observed to be −5.17 kcal/mol and −3.68 kcal/mol respectively. The $\boldsymbol{\Delta G^{\#}_{binding}}$ values of the polymer catalysts are given in Table 7. Relatively lower $\boldsymbol{\Delta G^{\#}_{binding}}$ of **C3** for Z-L-Phe-PNA probably reflected the formation of well-defined three dimensional memory cavities with L-configuration for the incorporation of the substrate.

The substrate affinity of **C3** is reflected mainly in the activation free energy of the shape-selective binding of substrate. The $\Delta\left(\Delta \boldsymbol{G^{\#}_{binding}}\right)$ facilitated binding of Z-L-Phe-PNA as compared with the D-form in the range of −1.49 (**C3**) to 0.031 (**P3e**) and 0.019 kcal mol^{-1} (**P3c**). Predominant reaction for the L-form of the substrate over the D-form was also reflected in the difference of activation free energy of $\Delta\left(\Delta \boldsymbol{G^{\#}_{[C.S]}}\right)$ for the reaction process; $\Delta\left(\Delta \boldsymbol{G^{\#}_{[C.S]}}\right)$ values observed were −1.27, −0.012 and −0.019 kcal mol^{-1} for the polymer catalysts **C3**, **P3c** and **P3e**. As a result, the substrate stereospecificity of the highly competent **C3** catalyst is reflected mostly by the activation free energy of the stereospecific substrate-binding in the recognition site in the polymer catalyst and to a certain extent by the stereospecific reaction in the catalyst–substrate complex.

Even though 20% EGDMA crosslinked polymers **P3c** and **P3e** obey Michaelis-Menten kinetics, the lack of substrate stereoselectivity can be explained as due to the incorporation of both D- and L-TSA molecules along with the achiral monomers in the PPC. The chirality of the print molecule along with chiral monomers bestowed enhanced enantioselectivity on **C3**. The CT mimic **C3** is found to be 9.64 times stereoselective than **P3e** due to the presence of stereoselective L-cavity furnished by L-TSA-L-Mono*mer* pre-polymerization complex during TSA imprinting, which selectively binds L-PNA over D-PNA.

Table 7
Kinetic parameters supporting substrate stereospecificity of the polymer catalysts.

Polymercatalysts	k^L_{acc}/k^D_{acc}	K^D_m/K^L_m	$\Delta G^{\#}_{binding}$ (kcal/mol)		$\Delta\left(\Delta G^{\#}_{binding}\right)$	$\Delta\left(\Delta G^{\#}_{[C.S]}\right)$
			L-PNA	D-PNA		
C3	7.56	10.59	−5.17	−3.68	−1.49	−1.27
P3c	1.02	1.03	−4.13	−4.09	−0.019	−0.012
P3e	1.03	1.05	−4.26	−4.23	−0.031	−0.019

Allkineticparameters within the limit ±5%.

Table 8
Influence of chiral amino acid monomers and achiral organic monomers on substrate specificity of polymer catalysts.

Kineticparameter	C3	P3c	P3e
k^{Phe}_{acc}	123.78	60.54	66.54
k^{Tyr}_{acc}	108.58	51.09	55.39
k^{Trp}_{acc}	24.86	11.35	14.45
k^{Ala}_{acc}	19.43	9.15	9.65

Allkineticparameters within the limit ±5%.

Table 9
Influence of chiral amino acid monomers and achiral organic monomers on substrate shape-selectivity of polymer catalysts.

Selectivity ratio	P3c	P3e	C3
k^Z_{acc}/k^{Boc}_{acc}	2.56	3.18	4.56
k^Z_{acc}/k^{Fmoc}_{acc}	4.21	4.83	8.21
$k^Z_{acc}/k^{Nphth}_{acc}$	8.04	8.85	14.24

All kinetic parameters within the limit ±5%.

3.8. Substrate specific amidolysis of P3c and P3e

The substrate-specificity 'the discrimination of a substrate over other competing molecules' of the TSA-built polymer catalysts **P3c** and **P3e** towards chymotrypsin specific and non-specific amino acids was investigated [19,20,31,32]. The mimics showed higher specificity towards Z-L-Phe-PNA and Z-L-Tyr-PNA. But the specificity towards Phe is slightly higher than Tyr (Table 8**)**. However, the mimics **P3c** and **P3e** exhibited almost half the specificity of **C3**. The mimics showed reduced specificity towards Trp, which is a chymotrypsin specific amino acid. The rate acceleration k^{Trp}_{acc} values observed are 24.86 (**C3**), 11.35 (**P3c**) and 14.45 (**P3e**). The lower k^{Trp}_{acc} values are due to the incompatibility of the indole ring in the catalytic cavity. The substrate Ala-PNA was found to be non-specific to the mimics. Like natural chymotrypsin, the mimics are also found to be non-specific towards Ala-PNA.

3.9. Substrate shape-selective amidolysis

The substrate-recognition ability of TSA imprinted polymer catalysts **P3c** and **P3e** was investigated using phenylalanine *p*-nitroanilides with various N^{α}-protecting groups like benzyloxylcarbonyl(Z), N-t-butyloxycarbonyl (Boc), 9-fluorenylmethoxycarbonyl (Fmoc) and N-phthaloyl (Nphth) [27]. The mimics kept the structure of the imprinted TSA with benzyloxycarbonyl group in memory and recognized the structure of Z-L-Phe-PNA and shape-selectively accommodated it in the catalytic cavity. The substrate selectivity is observed in the order Z > Boc > Fmoc > Nphth-L- Phe-PNAs. The capacity of the mimic to recognize the structure of the protecting group was evaluated as shape-selectivity, in terms of the ratio k^Z_{acc}/k^{Boc}_{acc}, k^Z_{acc}/k^{Fmoc}_{acc} and $k^Z_{acc}/k^{Nphth}_{acc}$. The shape-selectivity ratios were evaluated; compared with the substrate shape-selective stabilization power of **C3**. The k_{acc} values calculated for the mimic **P3c** were found to be 60.54 (Z-L-Phe-PNA), 23.65 (t-Boc-L-Phe-PNA), 14.38 (Fmoc-L-Phe-PNA) and 7.53 (Nphth-L- Phe-PNA). For the mimic **P3e** the corresponding values are 66.54, 20.92, 13.78 and 7.52. The substrate shape-selectivity ratios exhibited by the polymer catalysts are recorded in Table 9. The maximum substrate-shape selectivity is observed between Z and Nphth-L-Phe-PNAs and the selectivity $k^Z_{acc}/k^{Nphth}_{acc}$ value was 8.04 for **P3c** and 8.85 for **P3e**. But, for the mimic **C3**, the selectivity $k^Z_{acc}/k^{Nphth}_{acc}$ value was 14.24.

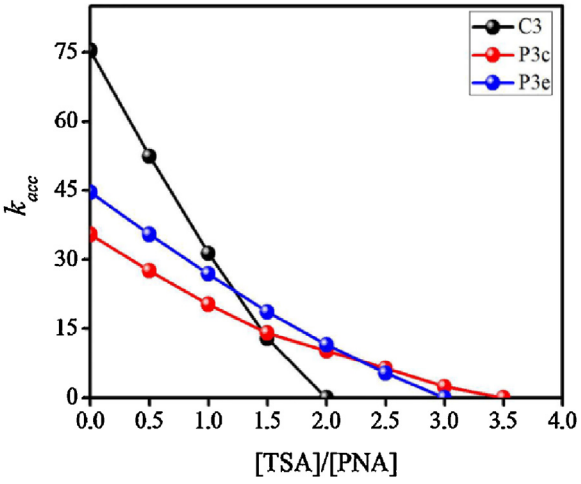

Fig. 10. TSA inhibition on the amidase activity of **C3**, **P3c** and **P3e**.

3.10.TSA inhibition study

A typical property of enzymes is the inhibition by certain molecules. A transition-state analogue imprinted polymer should show competitive inhibition by the template [6,33,34]. The TSA inhibition studies were carried out in the amidolytic reaction in presence of the imprinted phosphonate TSA using the polymer catalysts **P3c**, **P3e** and **C3**.

As shown in Fig. 10, as the concentration of the template TSA increases, the amidase activity of the imprinted polymers was found to be fairly inhibited and then finally gets stopped. This results may be explained as due to "the shape-selective rebinding" of the imprinted TSA over the substrate **Z-L-Phe-PNA**. A better rebinding within shorter time is observed for **C3** due to the exact geometry of the imprinted TSA in the polymer matrix. This would be a further proof for catalysis to occur inside the imprinted cavity.

3.10. Comparison with natural chymotrypsin

The kinetics of amidolysis of Z-L-Phe-PNA catalyzed by trifunctional mimics **P3c** and **P3e** synthesized from organic analogues of amino acid monomers was compared with the amidolysis catalyzed by natural chymotrypsin, **CT** and the mimic **C3** made up of methacrylated amino acid monomers (Fig. 11).

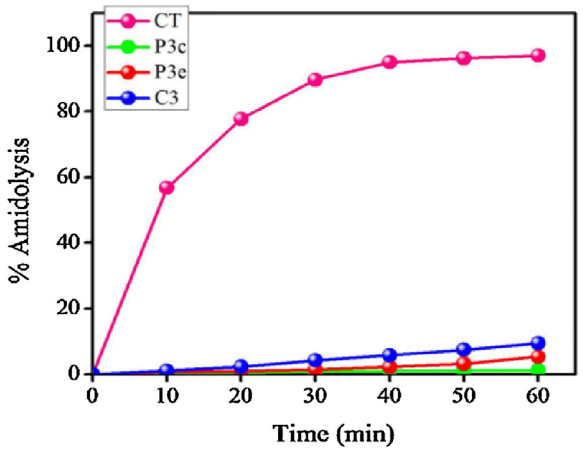

Fig. 11. % Amidolysis using natural chymotrypsin **CT** and trifunctional mimics **P3c**, **P3e** and **C3**.

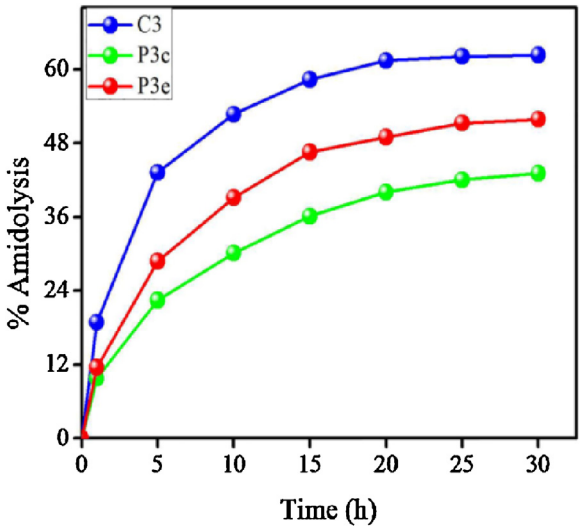

Fig. 12. % Amidolysis using **P3c**, **P3e** and **C3**.

With natural chymotrypsin, the amidolytic reaction reached 80% completion in 45 min. Michaelis-Menten behaviour of **P3c, P3e** and **C3** is not significant in the initial period of the amidolytic reaction. Compared to the natural enzyme, the poor rate of amidolysis exhibited by **P3c**, **P3e** and **C3** is due to the heterogenic nature of the reaction and the time required for the solvation of the polymer catalyst. The mimic **P3c** shows 40% completion of the reaction with a saturation time of 24 h and **P3e** shows 49.80% in 24 h. The enzyme mimic **C3** showed 62% completion of the reaction with a saturation time of 22 h (Fig. 12). The K_m value of chymotrypsin catalyzed amidolysis at room temperature was evaluated as 0.1 μm which is 14.19×10^3 times the value of the mimic **P3c**, 11.51×10^3 times the value of the mimic **P3e** and 2.7×10^3 times the value of the mimic **C3** at 45 °C.

Even though lower catalytic efficiency is exhibited by the imprinted mimics, the higher thermal stability, regeneration and reusability even after several cycles of experiments and years of higher shelf-life make them economic and superior over natural chymotrypsin.

The incubation studies showed that the trifunctional enzyme mimic **C3** is thermally stable up to 130 °C and further increase in temperature decreased its amidase activity. The mimics **P3c** and **P3e** are found to be stable up to 100 °C only. Further, the reduction in catalytic activities after regeneration and reusability was much more in the case of polymers derived from organic monomers. The results show that the cavities in the catalysts **P3c** and **P3e** get deformed easily than **C3**.

4. Conclusion

Polymer catalysts with the imprints of phenyl-1-(N-benzyloxycarbonylamino)-2-(phenyl)ethyl phosphonate were made up of achiral organic monomers and L- amino acid monomers to mimic natural chymotrypsin. The polymers derived from L-amino acid monomers are found to be substrate stereospecific. But the catalysts synthesized from organic monomers possess both L-and D-cavities in the polymer matrix and hence exhibited no enantioselectivity. Imidazole group of histidine residue/vinylimidazole monomer is the essential catalytic group in the active site of the mimics as in the case of hydrolase protein chymotrypsin. Allyl alcohol showed poor nucleophilicity in the amidolytic reaction. The pyridine moiety is capable of exerting H-bonding interaction with carboxyl group of methacrylic acid and π- stacking interaction with aromatic side chain of amino acid residue of the substrate *p*-nitroanilide. For the polymers derived from organic monomers, the rate enhancement and enzyme-like behaviour are observed, in the lower range of crosslink density (20 mol%). The thermal stability and recycling ability of these mimics were lower than the trifunctional mimic from amino acid monomers, but higher than natural chymotrypsin.

Acknowledgements

The authors gratefully acknowledge the support from Council of Scientific and Industrial Research (CSIR), India for awarding junior and senior research fellowships to Divya Mathew. We are also thankful to IIRBS, Mahatma Gandhi University, Kottayam, Kerala, India for providing facilities for spectral analysis and School of Biosciences, Mahatma Gandhi University for providing facilities for incubation studies.

References

[1] G. Wulff, J. Liu, Acc. Chem. Res. 45 (2012) 239–247.
[2] L. Chen, S. Xu, J. Li, Chem. Soc. Rev. 40 (2011) 2922–2942.
[3] G. Wulff, Chem. Rev. 102 (2002) 1–27.
[4] C. Alexander, L. Davidson, W. Hayes, Tetrahedron 59 (2003) 2025–2057.
[5] B.S. Lele, M.G. Kulkarni, R.A. Mashelkar, React. Funct. Polym. 39 (1999) 37–52.
[6] D.K. Robinson, K. Mosbach, J. Chem, Soc. Chem. Commun. (1989) 969–970.
[7] K. Ohkubo, Y. Urata, K. Yoshinaga, Polymer 35 (1994) 5372–5374.
[8] T. Sagawa, K. Togo, C. Miyahara, H. Ihara, K. Ohkubo, Anal. Chim. Acta 504 (2004) 37–41.
[9] B. Sellergren, R.N. Karmalkar, K.J. Shea, J. Org. Chem. 65 (2000) 4009–4027.
[10] J.-M. Kim, K.-D. Ahn, G. Wulff, Macromol. Chem. Phys. 202 (2001) 1105–1108.
[11] J.-M. Kim, K.-D. Ahn, A.G. Strikovsky, G. Wulff, Bull. Korean Chem. Soc. 22 (2001) 68–692.
[12] Y. Kawanami, T. Yunoki, A. Nakamura, J. Mol. Catal. A: Chem. 145 (1999) 107–110.
[13] D. Mathew, B. Thomas, K.S. Devaky, J. Mol. Catal. A: Chem. 415 (2016) 65–73.
[14] C.G. Overberger, T.St. Pierre, N. Vorchheimer, J. Lee, S. Yaroslavsky, J. Am. Chem. Soc. 87 (1969) 296–298.
[15] K. Ohkubo, Y. Urata, S. Hirota, J. Mol. Catal. 87 (1994) L21–L24.
[16] A. Leonhardt, K. Mosbach, React. Polym. 6 (1987) 285–290.
[17] B. Sellergren, K.J. Shea, Tetrahedron: Asymmetry 5 (1994) 1403–1406.
[18] J.-T. Haung, S.-H. Zheng, J.-Q. Zhang, Polymer 45 (2004) 4349–4354.
[19] K.A. Koehler, G.E. Lienhard, Biochemistry 10 (1971) 2477–2483.
[20] T.A. Steitz, R. Henderson, D.M. Blow, J. Mol. Biol. 46 (1969) 337–348.
[21] D. Carboni, K. Flavin, A. Servant, V. Gouverneur, M. Resmini, Chem. Eur. J. 14 (2008).
[22] R. Say, M. Erdem, A. Ersoz, H. Turk, A. Denizli, Appl. Catal. A: Gen. 286 (2005) 221–225.
[23] A. Visnjevski, E. Yilmaz, O. Brüggemann, Appl. Catal. A: Gen. 260 (2004) 169–174.
[24] G. Wulff, T. Gross, R. Schonfeld, Angew. Chem. Int. Ed. Engl. 36 (1997) 1962–1964.
[25] K. Golker, I.A. Nicholls, Eur. Polym. J. 75 (2016) 423–430.
[26] K. Ohkubo, K. Sawakuma, T. Sagawa, Polymer 42 (2001) 2263–2266.
[27] K. Ohkubo, K. Sawakuma, T. Sagawa, J. Mol. Catal. 165 (2001) 1–7.

[28] B.S. Lele, M.G. Kulkarni, R.A. Mashelkar, React. Funct. Polym. 40 (1999) 215–229.
[29] B.S. Lele, M.G. Kulkarni, R.A. Mashelkar, Polymer 40 (1999) 4063–4070.
[30] M. Danielle, D.A. Spivak, Org. Lett. 16 (2014) 1402–1405.
[31] K. Ohkubo, Y. Funakoshi, Y. Urata, Chem. Commun. 20 (1995) 2143–2144.
[32] K. Ohkubo, Y. Urata, S. Hirota, Y. Funakoshi, T. Sagawa, S. Usui, K. Yoshinaga, J. Mol. Catal. 101 (1995) L111–L114.
[33] K. Ohkubo, Y. Funakoshi, T. Sagawa, Polymer 37 (1996) 3993–3995.
[34] K. Ohkubo, Y. Urata, S. Hirota, J. Mol. Catal. 93 (1994) 189–193.